

## A Proposal for Safe and Profitable Enhanced Geothermal Systems in Hot Dry Rock

Luke P. Frash, J. William Carey, Bulbul Ahmmed, Matthew Sweeney, Meng Meng, Wenfeng Li, Bijay K C, Uwaila Iyare  
Los Alamos National Laboratory, Los Alamos, NM 87544  
lfrash@lanl.gov

**Keywords:** Uncertainty Quantification, GeoDT, Net Present Value, Fracture Caging, EGS

### ABSTRACT

The contemporary approach to developing hot dry rock (HDR) Enhanced Geothermal Systems (EGS) is, at its core, the same today as how it was first envisioned for the 1977 Fenton Hill project. During the past four-plus decades since Fenton Hill, the geothermal community has developed increasingly sophisticated coupled process models and deployed numerous pilot projects to quantify and seek solutions to the many challenges of contemporary EGS. However, this effort appears to be leading toward the conclusion that the contemporary approach is not economic and is unlikely to become economic without the advent of technology breakthroughs. Most critically, the achievable flow rates with conventional ‘traffic-light’ protocol to prevent induced seismicity are far too low for economic power generation. Adding to the challenge, subsurface processes for cold fluid-flow through closed heterogeneous fractures tend to encourage early thermal breakthrough and reduce production capacity. In this study, we employ our Geothermal Design Tool (GeoDT) to evaluate an alternative approach to EGS development that uses only current technologies to achieve economic geothermal power production from HDR resources. This work reveals a promising multi-well approach that could use: (1) ‘limited-entry’ for injection-well zonal flow-control, (2) ‘fracture caging’ for seismicity control, (3) high-rate and high-pressure injection for ‘hydropropping’, and (4) systems engineering that accommodate decreasing production well enthalpy over time. Our numerical models based on the Utah FORGE location indicate that this new alternative approach to HDR-EGS holds promise for reliable economic geothermal power generation, but more work is needed to demonstrate its effectiveness in field applications.

### 1. INTRODUCTION

Are we asking the right questions for how to make Enhanced Geothermal Systems (EGS) work? For the most part, the modern approach to developing EGS is the same now as how it was first envisioned for the Fenton Hill project (Brown et al., 2012). This conventional approach to development involves: (1) identifying and characterizing a resource, (2) drilling an injection well and stimulating the rock, (3) intercepting the stimulated rock volume with one or more production wells, (4) circulating water from the injection wells to the production wells for heat mining and power production, and (5) monitoring seismicity and reducing flow rates when seismicity exceeds predefined thresholds. While conceptually intuitive, this approach prefers subsurface characterization to an unachievable high level of detail and it is victim to crucial irreducible uncertainties with respect to seismic risk forecasting (Majer et al., 2012; Langenbruch et al., 2018). When creating a reservoir, uncertainty in the orientation of the in-situ stresses, the influence of unknown natural fractures and faults, and ambiguity between microseismic hypocenters and flowing fracture locations will lead to poor hydraulic connectivity and low flow rates (Frash et al., 2015). When circulating fluids for heat mining, proppant degradation and chemical precipitation are expected to decrease fracture permeability over time (Mattson et al., 2016) while chemical etching and thermal contraction lead to increased channelization by locally increasing permeability, all of which will hinder reservoir efficiency (Guo et al., 2016). For seismicity management, conventional traffic-light protocols are fundamentally reactionary without a method to accurately or reliably forecast risk. Instead, these protocols primarily aid the identification of induced versus natural seismic events. Furthermore, when traffic-light protocols trigger the reduction of flow rate, this action will lead to the loss of economic competitiveness for that geothermal system (Charléty et al., 2000; Richter, 2020). In general, efforts to improve contemporary EGS performance have included the pursuit of novel technologies for cost reduction, improving models to more accurately simulate complex coupled processes, or improving tools to characterize the subsurface so that stimulation and flow can be more fully controlled (Tester et al., 2006; Hamm et al., 2019). However, much of the uncertainty in the subsurface remains irreducible and key uncertainties remain unknowable with even the best foreseeable technologies, such as the unpredictable critical injection pressure that will trigger seismic fault slip.

To move forward with EGS development and its promise of abundant baseload clean energy, we propose a new question: Can we make HDR-EGS reliably economic using current technologies? When asking this question, it is crucial to also question the contemporary definitions of EGS and the associated assumptions of how EGS ‘should’ work, many of which date back to Fenton Hill. Based on experiences so far, the two most obvious needs for achieving economic EGS are: (1) specifiable flow rates for optimized power production are reliably safe, achievable, and much higher than what has been employed so far and (2) EGS designs that are tolerant of subsurface uncertainty and adaptive to what can happen so that the design will succeed often enough for the profit to overcome the risk. These two needs highlight that solutions to our proposed question must embrace uncertainty by considering the multitude of possibilities for complications that can happen in nature and the solution should offer the means to estimate the likelihoods of these possibilities.

Based on our learnings from experiments and models, our current hypothesis for how to economically produce power from hot dry rock EGS consists of four key elements (Fig. 1): (1) flow control in the injection wells to evenly distribute fluid among multiple stimulation zones; (2) reliable and direct control over injection-induced seismic risk by limiting the volume of stimulated rock; (3) uniform fracture propping that does not depend on proppants or shear stimulation; and (4) power systems that can accommodate reducing produced fluid

enthalpy over time that can vary from well to well. Our vision for the form of these key elements utilizes: (1) continuous ‘limited-entry’ injection, (2) ‘fracture caging’ verified by tracer testing, (3) ‘hydropropping’ where fractures are held open by high fluid pressure, and either (4a) modular power plant designs that adapt to decreasing well enthalpy and variable flow rate with minimal efficiency losses or (4b) a sequentially harvested reservoir with a production zone that changes over time to maintain more stable overall enthalpy, possibly through drilling new wells. In this study, we employ our Geothermal Design Tool (GeoDT) to investigate the economic potential of an EGS system that uses these combined concepts. The parameters for this study are based on Utah FORGE but include the options of more wells and deeper depths. To evaluate economic potential, we will estimate the net present value of each modeled realization by factoring in capital costs for the wells and the plant, maintenance costs, power generation, pumping costs, and crude model for the cost of inducing large seismic events. This economics module is included in the most recent release of our open-source code, GeoDT. The intent of this work is to explore the potential of EGS if we were to adopt new approaches to how this source of hot dry rock energy could be tapped for clean baseload power generation. As our model shows, there could be significant potential in alternative approaches to EGS but more work is needed to confidently refine and confirm, or refute, our predictions.

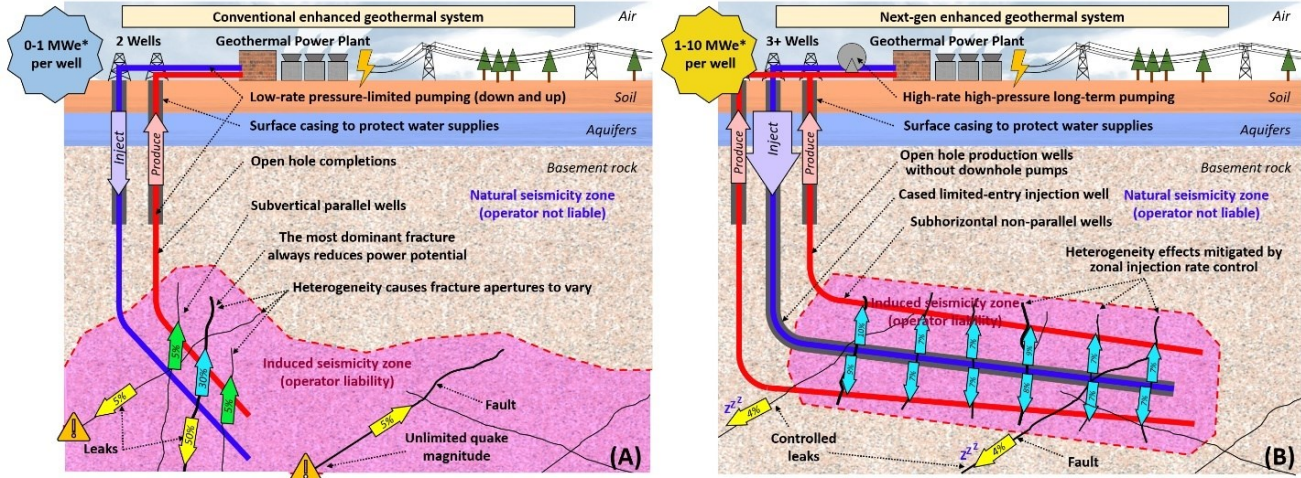


**Figure 1:** (a) The contemporary and historical EGS concept with two wells drilled sequentially compared to (b) our proposed multi-well EGS concept that uses ‘limited entry’ injection for flow control, ‘fracture caging’ for limiting seismic risk, ‘hydropropping’ for uniform fracture flow, and modular power to adapt to variable produced fluid enthalpy and rate.

## 2. GEOTHERMAL DESIGN TOOL

To address our question of how to economically develop EGS using current technologies, we developed a fast simplified multi-physics solver to evaluate EGS designs in uncertain geologic systems (Frash, 2021; Frash, 2022; Frash et al., 2022). We call this modeling tool the Geothermal Design Tool (GeoDT). By design, the architecture of this tool is numerically efficient enough to model thousands of realizations in a few hours using a desktop computer. Meanwhile, the underlying assumptions of this model are empirically based on laboratory and field data so that complex coupled processes are at least partially accounted for without needing to model these complex processes directly (Frash et al., 2021). The intent of this model is to run it with full uncertainty, as informed by a broad spectrum of relevant prior laboratory and field measurements, and to reduce the uncertainty only when suitable information is available. When a promising EGS design is identified, it can then be investigated in greater detail and at higher fidelity using other more powerful, but more expensive, numerical modeling codes. This study does not include the use of higher fidelity codes.

The primary features of GeoDT include (Fig. 2):

1. Pressure and flow rate prediction for 3D networks of intersecting wells and fractures that are modeled as pipes and nodes.
2. Hydraulic stimulation prediction with shear and tensile mechanisms where fracture apertures depend on effective stress.
3. Transient heat production predictions that depend on fluid enthalpy, rock conductivity, and stored energy change over time.
4. Electrical power generation using the combined single-flash Rankine and isobutane binary cycle.
5. Net present value prediction based on geothermal cost estimation tools, electricity sales, and a simple earthquake cost model.

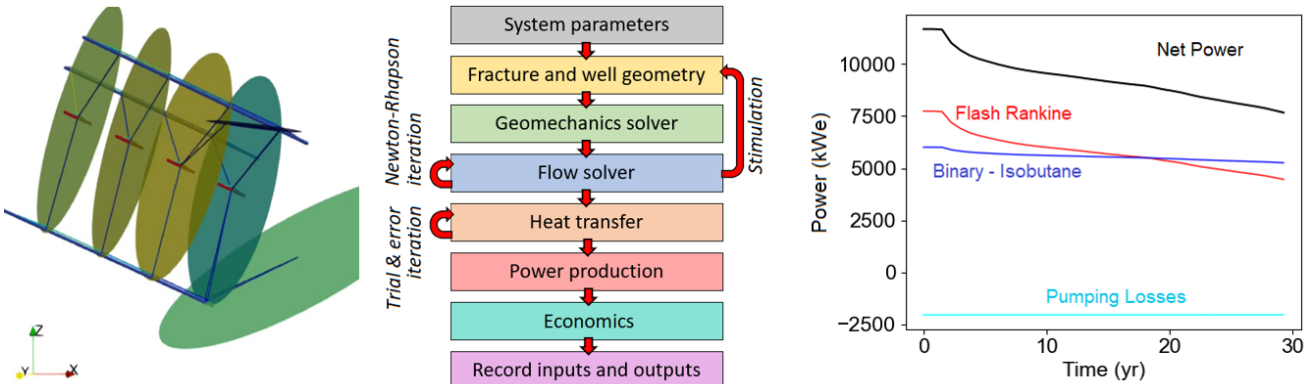


**Figure 2:** GeoDT stochastically predicts reservoir parameters, flow networks, hydraulic stimulation, heat production, power production, injection-induced seismicity potential, and ultimately net present value by fast and simplified methods. Most models complete in around 15 seconds using a single processor thread on a common desktop computer.

### 3. NET PRESENT VALUE ESTIMATION

Here, we introduce our economics module for GeoDT to estimate the net present value (NPV) of an HDR-EGS geothermal project. This module considers capital costs, maintenance costs, pumping costs, power sales, and injection-induced seismic risk. Following the theme of fast-simplified physics, our economics module uses simplified methods to estimate costs where the underlying goal is to give a conservative view of the economic potential of a project. Furthermore, the economics module yields a clear objective value for EGS design optimization, which progresses GeoDT towards its goal of informing HDR-EGS design decision making.

For well cost, we employ a cost per drilled length (USD/m) based on publicly available reports and models (Entingh et al., 2012; Lowry et al., 2017). Our baseline estimate for this cost is  $2763 \pm 536$  USD/m (Fig. 3), using the values for a 'large' 0.31 m diameter well with a horizontal liner from Lowry et al. (2017). To obtain this value as a price per drilled length, we excluded Lowry et al.'s (2017) 590,000 USD fixed cost for the well pad, rig mobilization, and miscellaneous expenses. Instead, this fixed cost is included in the capital cost for our economics model. Furthermore, we anticipate cost savings for our proposed multi-well EGS concept because all wells are planned to be drilled from a single pad during a single rig deployment with minimized downtime. This drilling method yield faster average drilling rates, improves the likelihood of successful fracture caging, and enables use of industry best-practices for optimizing drilling cost. To confirm our estimate, we also estimated drilling costs at  $2690 \pm 651$  USD/m using the GETEM model (Entingh et al., 2012) assuming EGS scenarios at 2 to 5 km depth and resource temperatures ranging from 175 to 350 °C.

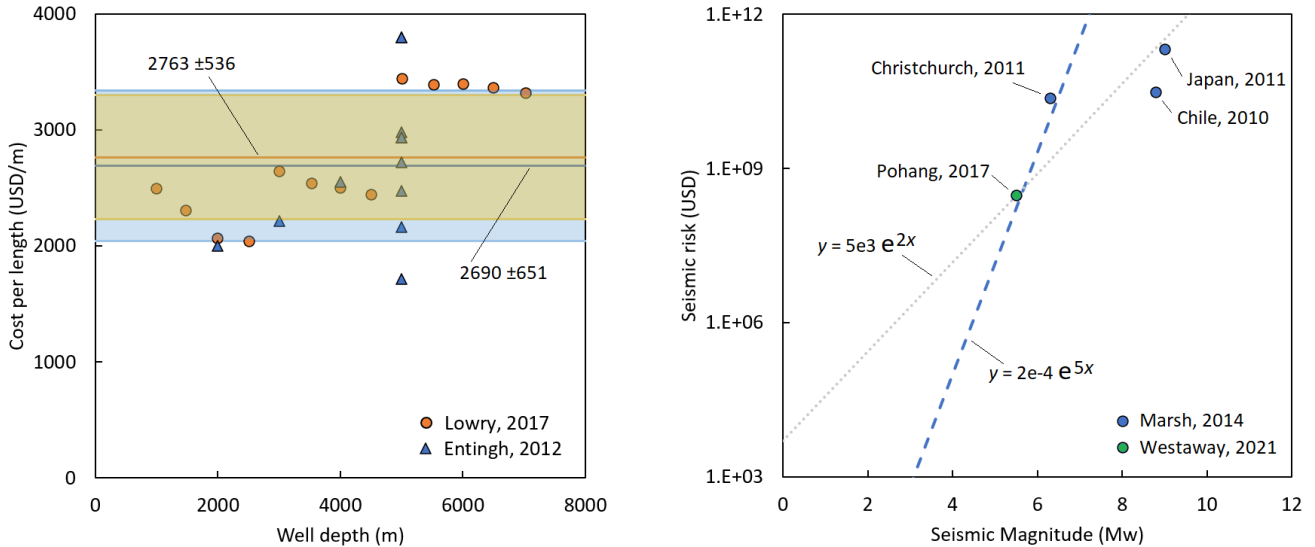


**Figure 3:** Cost models (left) for drilling cost per length of well based on GeoVision and GETEM (Lowry et al., 2017; Entingh et al., 2012) and (right) for seismic risk based on insurance claims from severe earthquakes (Marsh, 2014; Westaway, 2021).

Next for seismic risk, any quantitative assessment will be ambiguous, inherently unreliable, and sensitive to site specific context. For example, earthquake damage potential will depend on the regional geology (e.g., soft alluvium versus stiff bedrock), proximity to population centers (e.g., cities), proximity to critical infrastructure (e.g., dams, railroads, and hospitals), and mismatch between historic seismic risk and elevated injection-induced seismic risk with respect to building codes (e.g., Oklahoma). An economic risk estimate that has these concerns included is beyond the scope and purpose of GeoDT. Instead, we explore historical data for insurance claims from catastrophic earthquakes near dense population centers to obtain a high-penalty estimate of potential cost (Marsh, 2014; Westaway, 2021; Fig. 3). Here, we seek the most expensive earthquakes in recent history in order to obtain a pessimistic first-order estimate of

economic hazard as a function of seismic magnitude. To estimate the probability of a given magnitude earthquake occurring, we utilize the ‘maximum possible quake’ prediction from the GeoDT hydraulic stimulation model. This GeoDT model combines Gutenberg-Richter magnitude-frequency distributions with modeled fault radii, oriented shear stress state, rock stiffness, and stress-drop to estimate the largest earthquakes that could be induced at the modeled EGS site. This approach is similar to estimating seismic risk from the dimensions of known active faults but the underlying causal mechanism in our model is fluid injection. This makes our model more suitable for predicting ‘fracture caging’ to limit seismic magnitudes (Frash et al., 2020). This framework led us to an exponential cost model with a coefficient of 0.0002 USD and an exponent of  $5.0 \text{ Mw}^{-1}$ . Here, we note that damaging induced seismicity at any EGS site could harm public acceptance for EGS technology, so we desire a model that assumes arguably obnoxious penalties to events of around 4.5 or larger because we deem these events to be impermissible.

The remainder of our economics module’s terms are obtained from Lowry et al. (2017) and GETEM (Entingh et al., 2012) following a similar approach to the well cost per length estimate. We summarize these cost factors in Table 1. Our sales and costs best reflect the time from 2010 to 2020 and are therefore likely to be low compared to 2023 due to the ongoing supply chain disruptions, inflation, and rising energy costs. Unlike the stochastic reservoir and design parameters in Table 2, the economics analysis in this study uses only the constant “model’s value” from Table 1 and ignores economic uncertainty because it is not beneficial to HDR-EGS design optimization.

**Table 1: Summary of cost terms in the economics module of GeoDT.**

Parameter	Unit	Model’s Value	Uncertainty	Reference
Electricity sales per kilowatt-hour	USD/kWh	0.1372	-0.056 / +0.166	EIA, 2022
Drilling cost per length	USD/m	2763	$\pm 536$	Lowry et al., 2017
Drill pad cost	kUSD	590	-590 / +2,000?	Lowry et al., 2017
Power plant cost	USD	2026	$\pm 373$	GETEM
Exploration cost per depth	USD/m	2683	$\pm 472$	GETEM
Operating cost per kilowatt-hour	USD/kWh	0.0365	$\pm 0.0079$	GETEM
Seismic risk coefficient	USD	0.0002	1e-8 to 1e-3	This paper with 5.0 exponent
Seismic risk exponent	1/Mw	5.0	2.0 to 5.5	This paper with 2e-4 coefficient

Relevant outputs from each GeoDT model that pair with these cost factors include the net power output ( $P_{out}$ ) for each model timestep  $ep$ , timestep parameters (TimeSteps and LifeSpan), reservoir depth (ResDepth) and well length (w\_length), number of production wells (w\_count), length ratio of the injection well to production wells (w\_proportion), and the ‘max possible quake’ (Max\_Quake). The net power production term ( $P_{out}$ ) additively combines flash cycle generation ( $F_{out}$ ), binary cycle generation ( $B_{out}$ ), and injection well pumping losses ( $Q_{out}$ ). Each power term includes thermodynamic cycle losses, fluid losses, and the nominal 85% turbomachinery efficiency term (GenEfficiency) for pumps and turbines. Complications arising from fluid loss, reservoir inefficiencies, poor well connectivity, fracture interactions, and stress-dependent fracture permeability are but a handful of examples for the many field-scale complications that GeoDT will predict and factor into the economic cost estimation. To explore this functionality, please refer to the open-source release of this code on GitHub ([github.com/GeoDesignTool/GeoDT](https://github.com/GeoDesignTool/GeoDT)).

#### 4. CASE STUDY BASED ON FORGE

We elect to use the FORGE project near Milford, Utah, as the basis for assessing our proposed method to achieve economic power production from HDR-EGS. This location is highly characterized with publicly available measurements and observations. This location also features a geothermal gradient of around  $85 \text{ }^{\circ}\text{C}/\text{km}$  which is much higher than the global average gradient of  $25 \text{ }^{\circ}\text{C}/\text{km}$  so this site could be considered a high-grade geothermal prospect. The complete list of parameters for our models are given in Table 2. Key variables for this study are: (1) the spacing between the injection well and the production well(s) and (2) the injection rate into each isolated interval of the injection well. In addition, we employed batch runs for nominally 2,500 realizations (Fig. 4) at discrete depths and for geothermal system designs that featured either 2, 3, 4, or 5 wells, including the lone injection well. All scenarios consider only one injection well with a geometry and orientation matching what was drilled for FORGE 16A(78)-32. Detailed explanation of each model term will not be provided in this paper. The documentation provides more information ([github.com/GeoDesignTool/GeoDT](https://github.com/GeoDesignTool/GeoDT)).

Contemporary EGS traffic-light protocol include injection pressure and flow rate limits to manage induced seismic risk by limiting reservoir pressures, however none of our models impose this limitation because they instead rely on ‘fracture caging’ to control seismic risk. While GeoDT can impose contemporary limits on pressure and rate boundary conditions, the associated flow in hydraulic fracture scenarios will always be uneconomic because GeoDT does not currently have propped tensile fractures implemented. With future updates and improvements to the code, we plan to add proppant effects to tensile fractures to maintain higher permeabilities than what our current GeoDT fracture model assumes to be possible for closed tensile fractures. Without this change to the code and the associated assumptions, GeoDT will only predict economic EGS flow rates in HDR scenarios that are lucky enough for naturally conductive or stimulate-able shear fractures to connect the wells to each other through more than one fracture and without short-circuiting. Adding propped fractures as a feature to GeoDT is planned for future work to help better contextualize our proposed approach to EGS development in comparison to contemporary approaches. In short, we anticipate that our single injection interval two-well scenarios will perform most similarly to the contemporary approach to EGS development where short circuiting has a high probability unless diverters or in-well tools are successfully developed to mitigate the short-circuiting problem.

**Table 2: Parameters used for our models, based on FORGE.**

Parameter	Unit	Value	Distribution	Source
Domain size (i.e., cubic side length)	m	1600	-	FORGE Native State Model
Nominal reservoir depth	m	2340 to 3860 +/-10	Uniform	GDR, 2020
Geothermal gradient	K/km	83.1 to 87.4	Uniform	Allis et al., 2018
Rock density	kg/m <sup>3</sup>	2550 to 2950	Uniform	FORGE Native State Model
Rock thermal conductivity	W/mK	1.78 to 3.32	Uniform	FORGE Native State Model
Ambient surface temperature	C	0	Uniform	Constant for this study
Lowsteam pesssure	MPa	0.101	-	Constant for this study
Cement thermal conductivity	W/mK	2	Uniform	Asadi et al., 2018
Cement volumetric specific heat capacity	kJ/m <sup>3</sup> K	2000	Uniform	Kodur, 2014
Turbomachinery efficiency	%	85	-	Constant for this study
Project lifespan	yr	30	-	Vitaller et al., 2020
Injection temperature	C	20 to 90	-	Variable for this study
Power plant inlet pressure	MPa	1	Uniform	Constant for this study
Thermal analysis timesteps	steps	41	-	Constant for this study
Casing inner radius	m	0.0889	Uniform	Rassenfoss, 2022
Casing outer radius	m	0.1016	-	Rassenfoss, 2022
Borehole radius	m	0.1143	-	Rassenfoss, 2022
Borehole thermal convection coefficient	kW/m <sup>2</sup> K	3	Uniform	Kosky et al., 2013
Hazen-Williams friction coefficient	-	80	Uniform	Jeppson, 1974
Water density for flow analysis	kg/m <sup>3</sup>	920 to 932	-	Cooper and Dooley, 2007
Water dynamic viscosity	cP	0.2	-	Huber et al., 2009
Reservoir pore pressure	MPa	21.3	Uniform	FORGE Native State Model
Rock elastic modulus	GPa	55 to 62	Uniform	FORGE Native State Model
Rock Poisson's ratio	m/m	0.26 to 0.4	Uniform	FORGE Native State Model
Minimum stress azimuth	deg	258 to 338	Uniform	Xing et al., 2020
Minimum stress dip	deg	-20 to 20	Uniform	Xing et al., 2020
Overburden stress	MPa	58.6 to 67.0	Uniform	Xing et al., 2020
Intermediate stress	MPa	34.1 to 52.6	Uniform	Xing et al., 2020
Minimum stress	MPa	31.9 to 46.9	Uniform	Xing et al., 2020
Well spacing	m	30 to 747.8	Uniform	Variable for this study
Well length	m	1113.9	Lognormal	GDR, 2020
Well azimuth	deg	1.833	Uniform	GDR, 2020
Well dip	deg	0.438	Uniform	GDR, 2020
Well count	wells	1 to 4	Uniform	Variable for this study
Well proportion	deg	0.5 to 0.9	Uniform	Variable for this study
Well phase	deg	270	Uniform	Vertically above 16A(78)-32
Well intervals	zones	1 to 6	Uniform	Variable for this study
Fracture set 1 count	fractures	0 to 35	Uniform	FORGE Native State Model
Fracture set 1 diameter	m	150 to 1500	Uniform	No data
Fracture set 1 strike	deg	96 +/- 8	Normal	FORGE Native State Model
Fracture set 1 dip	deg	80 +/- 6	Normal	FORGE Native State Model
Fracture set 2 count	fractures	0 to 60	Uniform	FORGE Native State Model
Fracture set 2 diameter	m	150 to 1500	Uniform	No data
Fracture set 2 strike	deg	185 +/- 8	Normal	FORGE Native State Model
Fracture set 2 dip	deg	48 +/- 6	Normal	FORGE Native State Model
Fracture set 3 count	fractures	0 to 15	Uniform	FORGE Native State Model
Fracture set 3 diameter	m	150 to 1500	Uniform	No data
Fracture set 3 strike	deg	35 +/- 8	Normal	FORGE Native State Model
Fracture set 3 dip	deg	64 +/- 6	Normal	FORGE Native State Model
Fracture Friction Angle	-	20 to 45	Uniform	FORGE Native State Model
Fracture Cohesion	MPa	1 to 6	Uniform	FORGE Native State Model
Natural fracture base hydraulic aperture	m	1e-8 to 1e-4	Uniform	Frash et al., 2021
Hydraulic aperture to dilation ratio	m/m	0 to 2	Special	Frash et al., 2021
Fracture compressibility	1/MPa	2e-9 to 1e-7	Normal	Frash et al., 2021
Shear displacement-dilation coefficient	m/m	0 to 0.8	Normal	Frash et al., 2021
Shear displacement-length coefficient	m/m	10^-3 to 10^-1.2	Exponential	Frash et al., 2021
Fracture roughness	-	0.062 to 1.0	Uniform	Frash et al., 2021
Circulation flowrate	m <sup>3</sup> /s	0.0005 to 0.1	Exponential	Variable for this study
Production well pressure rise	MPa	-10 to 2	Uniform	Variable for this study
Boundary hydraulic aperture	m	1e-4 to 1e-3	Uniform	Variable for this study
Hydraulic fracture cohesion	MPa	0.1 to 0.4	Uniform	Frash et al., 2021
Hydraulic fracture friction angle	deg	15 to 35	Uniform	Frash et al., 2021

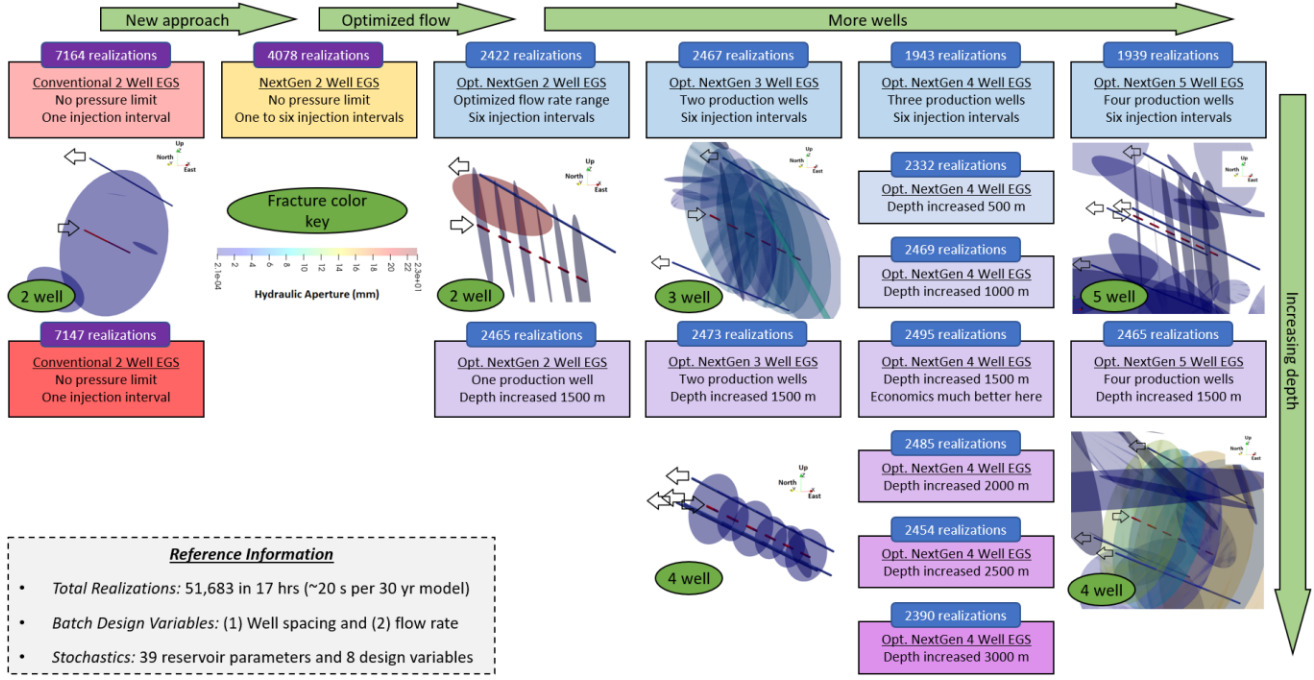


**Figure 4: Modeled matrix of 16 EGS design scenarios based on the FORGE site. Each scenario obtained more than 2,000 realizations to empower statistical assessment of the viability of each scenario for economic power generation. Larger numbers of realizations were produced for scenarios that considered larger ranges for the injection rate in order to have adequate sample sizes for post flow-optimization stochastic analysis. Each scenario included all steps of the modeling process from natural fracture placement through to long term heat production. This modeling work was conceived and completed within 24 consecutive hours, including model setup, execution, and results visualization.**

## 5. RESULTS

Our models yielded 51,683 realizations that included 3D well and fracture geometry (e.g., Fig. 4), timeseries data for each realization (e.g., Fig. 2), and summarized model inputs and key outputs. The example 3D results (Fig. 4) have arrows indicating the direction of flow into injection (red) and from production (blue) wells. Hydraulically tensile fractures radiating outward from the injection well were predicted for nearly 100% of the realizations. Hydroshear stimulation, with shear stimulation initiating from at least one of the injection well's intervals, was predicted for less than 2.5% of realizations. This low probability of shear-stimulation is a consequence of our sparse natural fracture network and the low-probability of intercepting a shear-critical and moderate-permeability natural fracture with the injection well (Meng et al., 2022). Further away from the injection well, natural fracture shearing triggered by the hydraulic fractures was quite common, occurring in around 20% of realizations. To make sense of our busy timeseries data (e.g., Fig. 5), we will first calculate the average net electrical power production and then estimate the net present value (NPV).

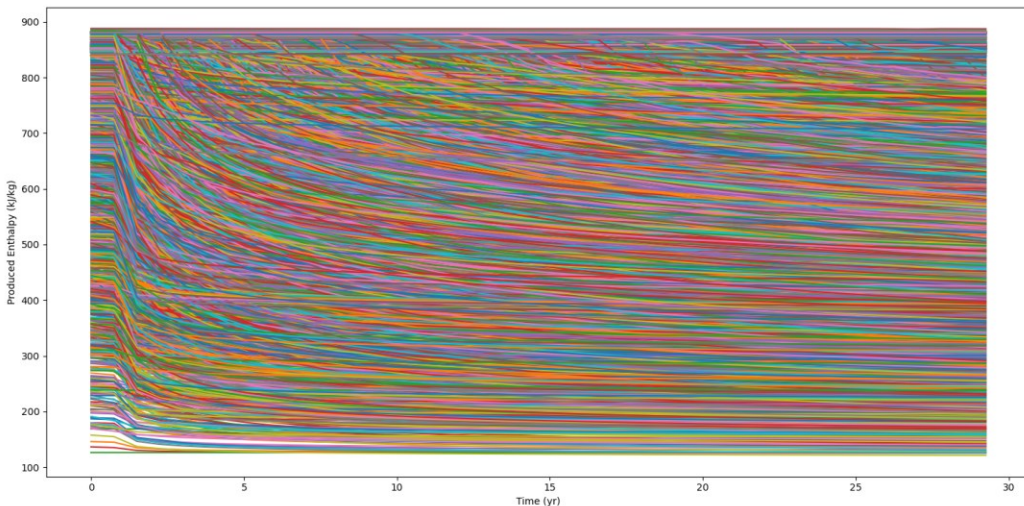


**Figure 5: Produced fluid enthalpy from 4078 realizations of the two well scenario with one to six injection intervals and injection rates ranging from 0.0005 to 0.10 m<sup>3</sup>/s. Nominal depth was 2350 m, equal to FORGE well 16A(78)-32. This result shows the temporal behavior of our models with thermal breakthrough predicted sometime between immediately and never.**

Before we focus on NPV, let's discuss the predicted net power output (Fig. 6) using the above two well scenario (Fig. 5). More specifically, we will investigate the average net produced power over a 30 yr production lifespan because the temporal power output based on enthalpy data decreases over time in most high-output scenarios. Effective actual power systems will seek to levelize the real-time well output to maximize utilization of surface equipment and to pair peak output with peak demand to maximize profits, but we do not include this detail in our analysis. Our results also show that allowing some decrease in well enthalpy, even within the first year of production, can be massively beneficial to producing more power overall. In many cases, peak power can be achieved when more than 10% cooling of the produced fluid is allowed. This result stems from the mechanism of greater heat flux (i.e., power transfer) to the working fluid in the subsurface when the thermal gradient between the rock and fluid (i.e., thermal drawdown) is larger. However, we acknowledge that this claim of beneficial thermal drawdown conflicts with the contemporary EGS approach where even minor thermal drawdown (i.e., thermal breakthrough) is thought to be a problem that needs to be avoided. Our results consistently demonstrate that early thermal breakthrough and allowing some thermal drawdown is advantageous for increasing net power production from EGS.

As the results show (Fig. 6), the produced power increases generally with increasing well spacing and increasing injection rate, but the scatter due to subsurface uncertainty dominates each individual realization. This model predicted behavior agrees with our expectations where the influence of natural fractures can strongly affect reservoir performance, positively or negatively. The predicted net power is most variable at injection rates greater than  $0.020 \text{ m}^3/\text{s}$  per isolated injection interval, with associated variability from less than  $-10 \text{ MWe/yr}$  to  $+10 \text{ MWe/yr}$  for the same EGS designs. Inspection of the corresponding 3D realizations indicates that this chaos at high injection-rates originates from surprise natural fractures and faults than can either hinder performance by short circuiting or leaking fluid or can boost performance by tapping into high-flow far-field hot water sources. Which of these circumstances occurs is determined merely by where these fractures happen to exist and whether they happen to be permeable. These details are not knowable before injection commences, but the severity of natural fracture effects is aggravated when injection rates are high.

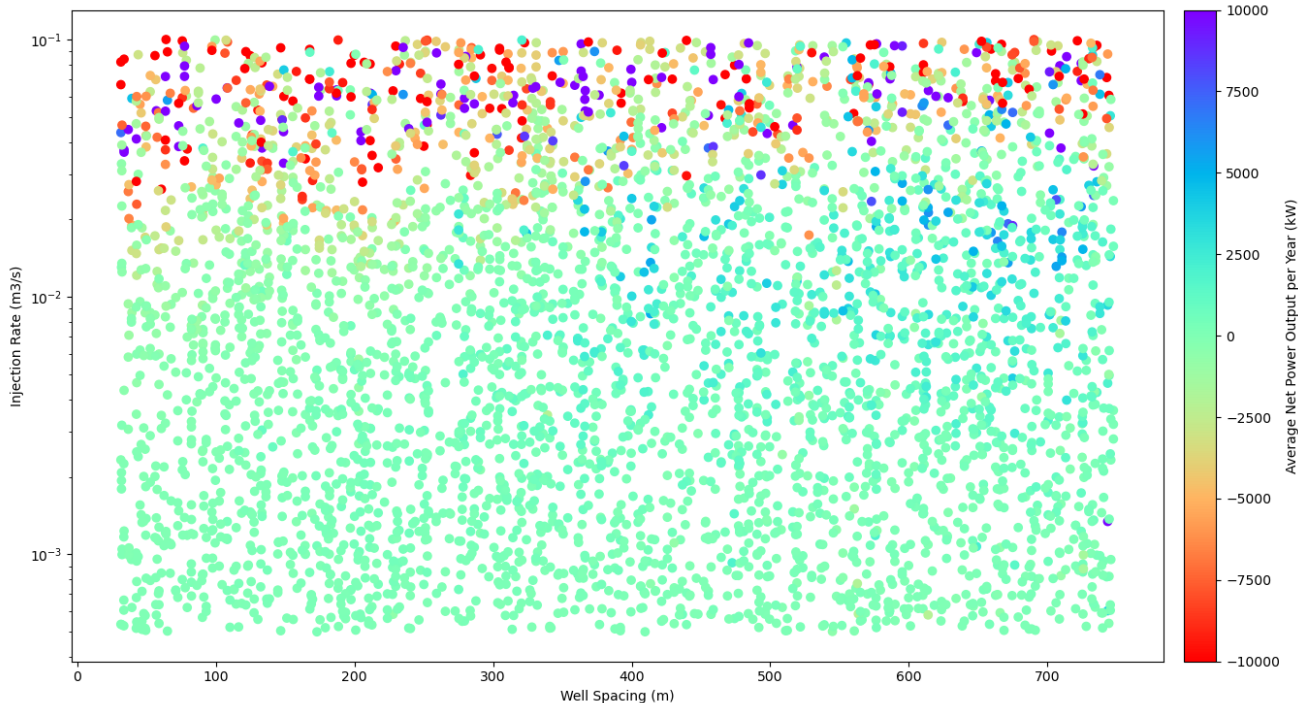


**Figure 6: Predicted net power output from the same 4078 realizations as a function of the first-order variables of injection rate per injection interval ( $Q_{inj}$ ) and well spacing ( $w_{spacing}$ ). This result shows a trend of low power at low flow rates (e.g.,  $< 0.001 \text{ m}^3/\text{s}$ ) and sporadic net produced power at high flow rates (e.g.,  $> 0.020 \text{ m}^3/\text{s}$ ). However, the more important detail is the underlying trend of increasing power with increasing flow rate and increasing well spacing.**

If we now investigate this same dataset from the perspective of NPV (Fig. 7), the underlying trend of increasing economic potential with increasing well spacing and increasing flow rate becomes clearer. As a reminder, the NPV metric calculates the relative benefit of power generation versus parasitic losses, capital costs, and seismic risk. Using NPV, we can identify a cluster of relatively stable and positive NPV in the middle-right of the plot. Positive NPV is generally predicted at an injection rate per interval of greater than  $0.005 \text{ m}^3/\text{s}$ . The values then become variable and risky at injection rates per interval greater than  $0.033 \text{ m}^3/\text{s}$ . In addition, an optimum flow rate as a function of well spacing is apparent, where increasing flow beyond the optimum causes excessive cooling and reduced productivity. We visually estimate the upper threshold for this optimum as a base-10 power function of well spacing with a coefficient of  $0.0005 \text{ m}^3/\text{s}$  and an exponent of  $0.003 \text{ m}^{-1}$ . Here, we seek to minimize the influence of the more obviously poor design decisions on our identification of the most promising HDR-EGS scenarios. Also, we seek to minimize the bias that can be introduced by over-fitting and the use of complex multi-parameter optimization algorithms. Therefore, all the forthcoming analysis to compare well design scenarios will apply the same thresholds as a filter to isolate the more logical EGS designs that will be more likely to succeed commercially.

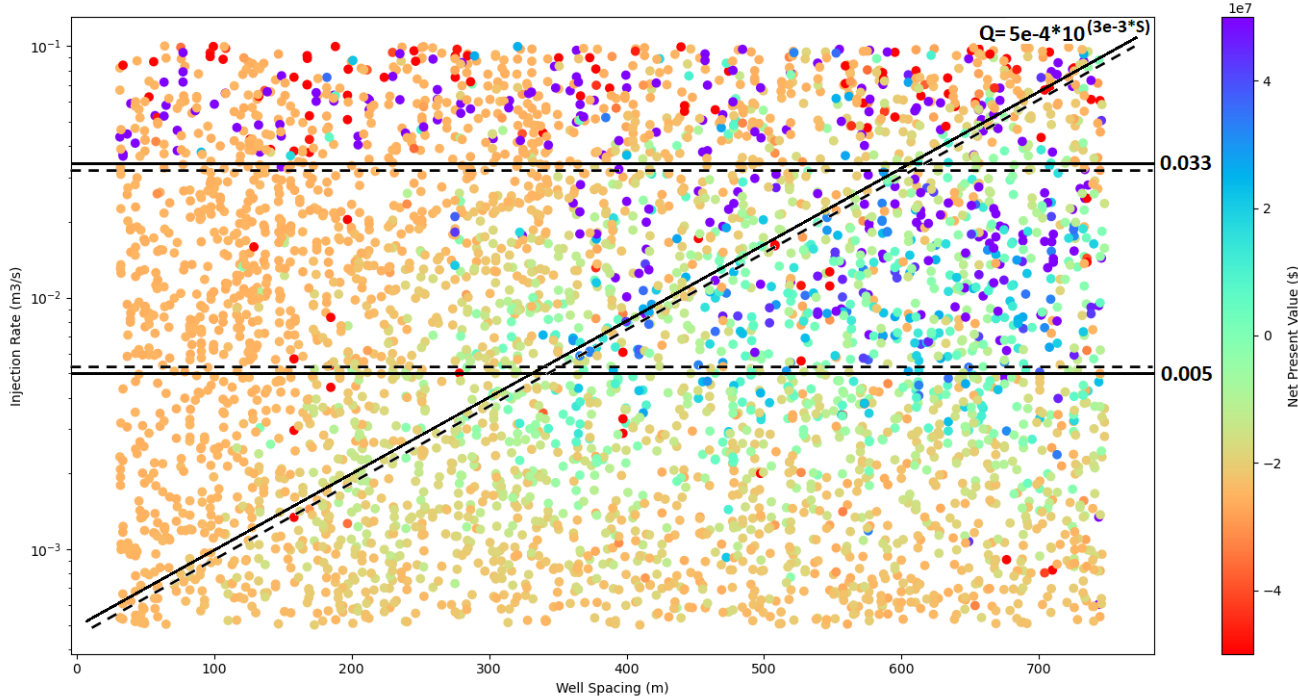


**Figure 7: Predicted net present values (NPV) of the base-case two-well design at Utah FORGE. This result abstractly shows that optimal injection rates for obtaining positive NPV is a function of well spacing and flow rate. To omit obviously poor design decisions for flow rates and spacing, we will filter all results to only the realizations having per-interval injection rates greater than  $0.005 \text{ m}^3/\text{s}$ , less than  $0.033 \text{ m}^3/\text{s}$ , and less than a function of  $5.0e-4 \times 10^{(3e-3 \times S)} \text{ m}^3/\text{s}$ , with  $S$  being well spacing. Injection slower than the lower limit will fail to realize the full potential of the resource. Injection faster than the upper limits increases the possibility of negative NPV due to seismicity and/or efficiency losses.**

Building on the NPV foundation, we will now estimate the P95, P90, P50, P10, and P05 metrics from each scenario after the flow rate and well spacing optimization filter was applied to each dataset. This filtering reduced each dataset to a nominal population of 1000  $\pm 500$  qualifying realizations. Adopted from the renewable energy business, the term “P95” signifies a value from the population where 95% of the remaining population has a higher NPV. Similarly, 50% of the population would have a value greater than “P50”. We seek EGS designs that will statistically reliably bring an NPV that is greater than zero, but risk tolerance will depend upon the perspective of an investor. This plot presents several exciting trends:

First, well cost is often the largest expense in an EGS project so there is a common assumption that decreasing the number of wells to a minimum is necessary to make a project economic. However, our result indicates that this common assumption could be incorrect. Instead, our models predict that increasing the well count tends to (1) increase containment of the injected fluid, (2) decrease seismic risk (Fig. 9), (3) increase total power production, and (4) delay thermal decline by sweeping fluid through a larger volume of hot rock. This trend is evident by comparing the 2w, 3w, 4w, and 5w scenarios at the depths of 2350 m (i.e., +0) and 3850 m (i.e., +1500).

Second, forcing injected fluid into multiple isolated injection intervals at nearly equal flow rates is predicted to be key to increasing overall power production and achieving a maximum NPV. This behavior was expected to be true prior to this study, but this study removes the injection rate and pressure limiter from conventional EGS designs by instead relying on ‘fracture caging’ to limit injection-induced seismic risk. Removing the pressure limit enables deployment of a ‘limited entry’ well system where flow is choked as it passes through the casing to impose a localized pressure drop. Complex fracture and flow dynamics introduced by this choke pressure drop can result in much more equal distribution of injected fluid among multiple injection intervals. Unlike low-pressure high-temperature flow control methods, this proven ‘limited entry’ technology is available today.

Third, this plot predicts that P50 NPV can be significantly positive, outpacing capital investment by a factor of 2 or more. If production was peaked during peak demand, the NPV could be raised higher than this model predicts. If direct use of the waste heat was also utilized for economic purposes (e.g., greenhouses, spas, or building heating), this NPV would undoubtedly rise even further. It is important to remember that this model is intended to be pessimistic and wholistic, but hopefully reasonable. This result provides an incentive to further investigate and validate our proposed concepts of (1) ‘limited entry’, (2) ‘fracture caging’, (3) ‘hydropumping’, and (4) power systems designed for variable enthalpy fluid or an expanding reservoir as feasible approach to HDR-EGS development.

Fourth, with respect to seismic risk, this result (Fig. 9) shows the potential value of having more wells in the ground to minimize seismic risk. These additional wells help to ensure against the possibility of natural fractures and faults intercepting flow, leaking, and then triggering large seismic events outside of the intended HDR-EGS reservoir. We hopefully exaggerated the penalty of seismic risk in our model by using our cost model (Fig. 3) that strongly discourages generating events larger than Mw 4.0.

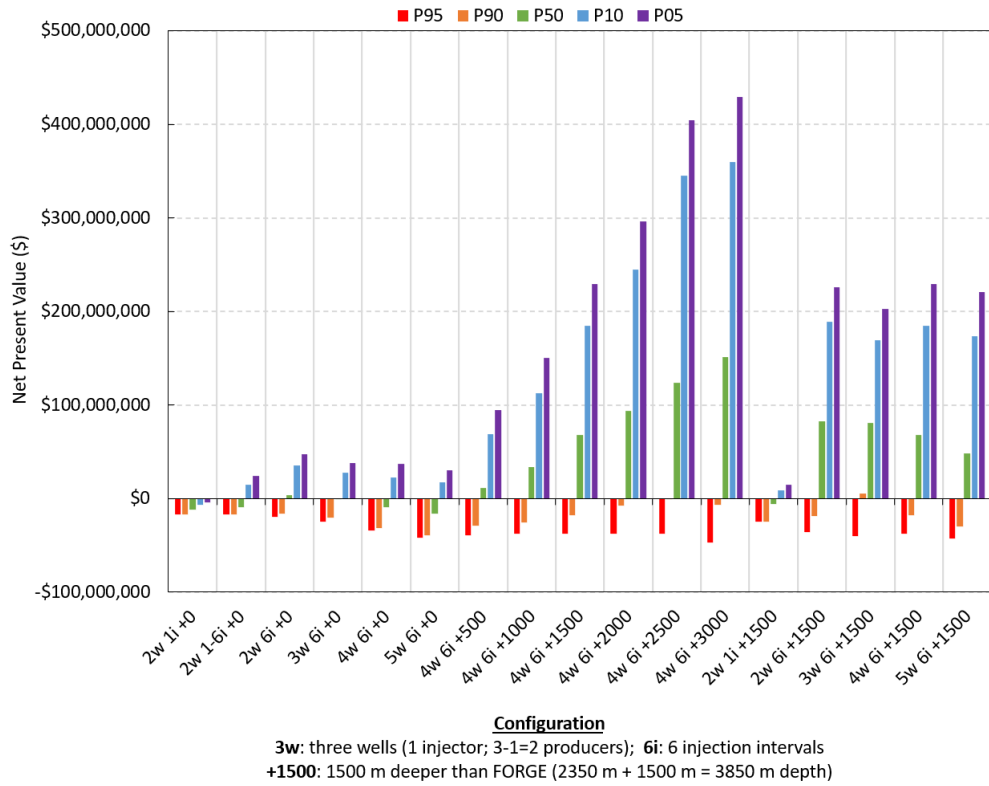


**Figure 8: Net Present Value (NPV) statistics for each scenario expressed using quantiles (e.g., P90). Our GeoDT model, subject to its limitations and assumptions, predicts that the FORGE site could become reliably profitable at depths greater than 3850 m where temperatures could be around 325 °C, assuming a constant geothermal gradient of 85 °C/km. Our models also predict that increasing the number of wells from two to three, four, or five will increase production from the site enough to effectively offset the capital costs of the additional wells.**

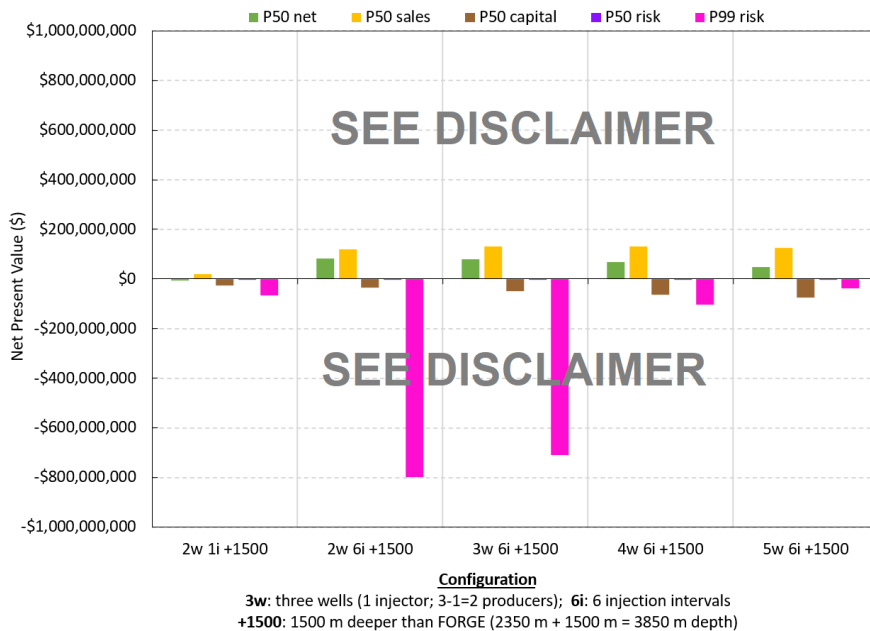


**Figure 9: Estimated sales, capital, seismic risk, and NPV as a function of well count and number of injection intervals at a depth of 3850 m. Increasing the number of injection intervals from 1 to 6 roughly coincides with increasing the total injection rate by a factor of 6. Increasing the number of production wells to at least four increases the likelihood that fracture caging will successfully prevent felt and/or damaging injection-induced seismicity. DISCLAIMER: THIS PLOT IS BASED ON VERY-HIGH ESTIMATES OF SEISMIC RISK FROM A NEW UNPROVEN MODEL. THIS IS NOT A PREDICTION FOR “FORGE” WHICH WILL HAVE (1) LOWER INJECTION RATES, (2) LOWER INJECTION VOLUMES, AND (3) SEISMICITY MITIGATION MEASURES THAT WE DID NOT MODEL.**

## 6. CONCLUSIONS

This study employed our rapid multi-physics Geothermal Design Tool (GeoDT) to explore a new approach to developing Hot Dry Rock (HDR) Enhanced Geothermal Systems (EGS). It took approximately 24 consecutive hours to setup, run, visualize, and analyze all of the 51,683 models for this study. This work included the study of 16 different scenarios with the goal of identifying an HDR-EGS design that could be commercially viable. These models were based on the Utah FORGE site and its first highly-deviated well 16A(78)-32. Our dataset is similar to the PIVOT 2022 Datathon example that is publicly available, but with an emphasis on considering more wells, deeper depths, and using Net Present Value (NPV) for the optimization objective. The most promising HDR-EGS designs employ: (1) a ‘limited entry’ well to evenly distribute injected fluid flow among multiple intervals, (2) ‘fracture caging’ to limit the risk of damaging injection-induced seismicity, (3) ‘hydropropping’ to sustain permeable tensile fractures in the subsurface without the need for propellant, and (4) an adaptive power systems design that could tolerate decreasing fluid enthalpy over time from each production well. With this design, we predicted that the 30 yr NPV could exceed the capital investment by more than a factor of two while simultaneously limiting injection-induced seismic risk. The most promising designs appear to require at least four wells, with more wells providing greater tolerance of subsurface uncertainty and reduced overall project risk. The body of this work discusses more insights that were gained from this effort, but which were beyond the scope of a conclusion. The models and analysis here feature a hypothetical alternative to the FORGE project where the goal is economic power production using currently available technologies. However, more work is needed to validate the ‘fracture caging’ and ‘hydropropping’ concepts that are a crucial component for reliably successful HDR-EGS designs, as predicted by our study.

## ACKNOWLEDGEMENTS

This work is supported by Department of Energy (DOE) Basic Energy Sciences under FWP LANL3W1. Additional support was provided by the Los Alamos National Laboratory’s Laboratory Directed Research and Development – Exploratory Research program (LDRD-ER-20220175ER). We are grateful for this funding provided by DOE and LANL.

The Python code for this work was developed using components from the “Fat Crayon Toolkit” (Singh et al., 2019) and was inspired by the EGS Collab Project (DOE-GTO). We gratefully acknowledge all the contributors to the Fat Crayon Toolkit, especially its lead developer Joseph P. Morris.

We also gratefully acknowledge critical and constructive feedback from J. William Carey, Pengcheng Fu, Meng Meng, and Wenfeng Li during discussions concerning the development of GeoDT.

## DISCLAIMER

This work employs low-accuracy methods to guess the maximum magnitudes of injection-induced seismicity with an intentional bias toward large events. The FORGE project uses low injection rates, low injection volumes, close well spacing, shallow depths, and many other mitigation measures to minimize injection-induced seismic risk.

## REFERENCES

Allis, R., Gwynn, M., Hardwick, C., Hurlbut, W., Moore, J.: Thermal Characteristics of the FORGE site, Milford, Utah, GRC Transactions (2018).

Asadi, I., Shafiq, P., Hassan, Z.F.B.A, and Mahyuddin, N.B.: Thermal conductivity of concrete - a review, Journal of Building Engineering, (2018).

Brown, D.W., Duchane, D.V., Heiken G., and Hriscu, V.T.: Mining the Earth's Heat: Hot Dry Rock Geothermal Energy, Springer: Verlag (2012).

Charléty, J., Cuenot, N., Dorbath, L., Dorbath, C., Haesslet, H., Frogneux, M.: Large earthquakes during hydraulic stimulations at the geothermal site of Soultz-sous-Forêts, International Journal of Rock Mechanics and Mining Sciences, 44 (8), 1091-1105 (2007).

Cooper, J.R. and Dooley, R.B.: Revised release on the IAPWS industrial formulation 1997 for the thermodynamic properties of water and steam, The International Association for the Properties of Water and Steam, (2007).

EIA: US Electricity Profile 2021, US Energy Information Administration (2022).

Entingh, D., Mines, G., Mansure, C., Petty, S., Nix, G., Augustine, C., Camp, E., Paster, M., Seungwook, M., Thodal, E., Hans on, S.: GETEM: Geothermal Electricity Technology Evaluation Model, Geothermal Technologies Office (2012).

Frash, L.P.: Optimized Enhanced Geothermal Development Strategies with GeoDT and Fracture Caging, Proceedings, 47th Workshop on Geothermal Reservoir Engineering, Stanford University, Stanford, CA (2022).

Frash, L.P.: Geothermal Design Tool (GeoDT), Proceedings, 46th Workshop on Geothermal Reservoir Engineering, Stanford University, Stanford, CA (2021).

Frash, L.P., Fu, P., Morris, J., Gutierrez, M., Neupane, G., Hampton, J., Welch, N., Carey, J.W., Kneafsey, T.: Fracture Caging to Limit Induced Seismicity, Geophysical Research Letters, 48(1), e2020GL090648 (2020).

Frash, L.P., Li, W., Meng, M., Carey, J.W., Sweeney, M.: Enhanced Geothermal System Design Using GeoDT and Fracture Caging — EGS Collab Stimulation Prediction Study, Proceedings, 56th US Rock Mechanics/Geomechanics Symposium, Santa Fe, NM (2022).

Frash, L.P., Welch, N.J., Meng, M., Li, W., Carey, J.W.: A Scaling Relationship for Fracture Permeability After Slip, Proceedings, 55th U.S. Rock Mechanics/Geomechanics Symposium, Virtual (2021).

Frash, L.P., Gutierrez, M., Hampton, J., Hood, J.: Laboratory simulation of binary and triple well EGS in large granite blocks using AE events for drilling guidance, *Geothermics*, 55, 1-15 (2015).

Guo, B., Fu, P., Hao, Y., Peters, C.A., Carrigan, C.R.: Thermal drawdown-induced flow channeling in a single fracture in EGS, *Geothermics*, 61, 46-62 (2016).

Hamm, S., et al.: GeoVision: Harnessing the Heat Beneath Our Feet, Department of Energy: Energy Efficiency and Renewable Energy, Geothermal Technologies Office (2019).

Huber, M.L., Perkins, R.A., Laesecke, A., and Friend, D.G.: New international formulation for the viscosity of H<sub>2</sub>O, *Journal of Physical and Chemical Reference Data*, (2009).

Jeppson, R.W.: Steady Flow Analysis of Pipe Networks: an Instructional Manual, Reports, 300, (1974).

Kodur, V.: Properties of concrete at elevated temperatures, *International Scholarly Research Notices*, (2014).

Kosky, P., Balmer, R., Keat, W., and Wise, G.: *Exploring Engineering*. Elsevier, (2013).

Langenbruch, C., Weingarten, M., Zoback, M.D.: Physics-based forecasting of man-made earthquake hazards in Oklahoma and Kansas, *Nature Communications*, 9, 3946 (2018).

Lowry, T.S., Finger, J.T., Carrigan, C.R., Foris, A., Kennedy, M.B., Corbet, T.F., Doughty, C.A., Pye, S., Sonnenthal, E.L.: GeoVision Analysis Supporting Task Force Report: Reservoir Maintenance and Development, Sandia National Laboratories, SAND2017-9977 (2017).

Majer, E., Nelson, J., Robertson-Tait, A., Savy, J., Wong, I.: Protocol for Addressing Induced Seismicity Associated with Enhanced Geothermal Systems, Department of Energy: Energy Efficiency and Renewable Energy, Geothermal Technologies Office, DOE/EE-0662 (2012).

Marsh & McLennan Companies: Comparing Claims from Catastrophic Earthquakes, Marsh Risk Management Research (2014).

Mattson, E., Neupane, G., Plummer, M., Jones, C., Moore, J.: Long-term Sustainability of Fracture Conductivity in Geothermal Systems using Proppants, *Proceedings, 41<sup>st</sup> Workshop on Geothermal Reservoir Engineering*. Stanford University, Stanford, CA (2016).

Meng, M., Frash, L.P., Li, W., Welch, N.J., Carey, J.W., Morris, J., Neupane, G., Ulrich, C., Kneafsey, T.: Hydro-Mechanical Measurements of Sheared Crystalline Rock Fractures With Applications for EGS Collab Experiments 1 and 2, *JGR Solid Earth*, 127 (2), e2021JB023000 (2022).

McLennan, J., Nash, G., Moore, J., Skowron, G.: 16A78-32 Summary of Daily Operations.pdf, Geothermal Data Repository, (2021).

Native State Modeling: Modeled Granitoid Parameters, <https://utahforge.com/laboratory/numerical-modeling/> (2022).

Rassenfoss, S.: Drillers vs. Granite: Hard Rock Is Losing Its Edge, *Journal of Petroleum Technology* (2022).

Richter, A.: New seismic event puts longer pause on geothermal project in Alsace, France, *Think Geoenergy* (2020).

Tester, J., Andersen, B.J., Batchelor, A.S., et al.: *The Future of Geothermal Energy*, Massachusetts Institute of Technology, ISBN: 0-615134386 (2006).

University of Utah: Utah FORGE Induced Seismicity Mitigation Plan, DE-EE0007080, University of Utah (2020).

Vitaller, A.V., Angst, U.M., and Elsener, B.: Laboratory tests simulating corrosion in geothermal power plants: influence of service conditions, (2020).

Well 16A78-32 Points Depths.csv, Geothermal Data Repository, (2020).

Westaway, R.: Extrapolation of populations of small earthquakes to predict consequences of low-probability high impact events: The Pohang case study revisited, *Geothermics*, 92, 102035 (2021).

Xing, P., McLennan, J., Moore, J.: In-Situ Stress Measurements at the Utah Frontier Observatory for Research in Geothermal Energy (FORGE) Site, *Energies* (2020).